

See discussions, stats, and author profiles for this publication at: <https://www.researchgate.net/publication/260910372>

# Direct Electrochemical Tyrosinase Biosensor based on Mesoporous Carbon and Co<sub>3</sub>O<sub>4</sub> Nanorods for the Rapid Detection of Phenolic Pollutants

ARTICLE · APRIL 2014

DOI: 10.1002/celc.201300208

---

CITATIONS

6

---

READS

64

4 AUTHORS, INCLUDING:



**Xue Wang**

Chinese Academy of Sciences

7 PUBLICATIONS 30 CITATIONS

SEE PROFILE



**XB Lu**

Dalian Institute of Chemical Physics

37 PUBLICATIONS 1,532 CITATIONS

SEE PROFILE



**Lidong Wu**

Chinese Academy of Fishery Sciences

17 PUBLICATIONS 72 CITATIONS

SEE PROFILE

# Direct Electrochemical Tyrosinase Biosensor based on Mesoporous Carbon and Co<sub>3</sub>O<sub>4</sub> Nanorods for the Rapid Detection of Phenolic Pollutants

Xue Wang,<sup>[a, b]</sup> Xianbo Lu,<sup>\*[a]</sup> Lidong Wu,<sup>[a, c]</sup> and Jiping Chen<sup>\*[a]</sup>

A novel tyrosinase (Tyr) biosensor based on a graphitized ordered mesoporous carbon/cobalt oxide nanorod (GMC/Co<sub>3</sub>O<sub>4</sub>) nanocomposite is developed for the rapid detection of phenolic pollutants. By applying the GMC/Co<sub>3</sub>O<sub>4</sub> nanocomposite as an enzyme immobilization matrix, rapid direct electron transfer between Tyr and the electrode is achieved. The biosensor exhibits a wide linear response for catechol, ranging from  $5.0 \times 10^{-8}$  to  $1.3 \times 10^{-5}$  M, with a limit of detection down to 25 nM and a response time of less than 2 s. The sensitivity of the biosensor based on the GMC/Co<sub>3</sub>O<sub>4</sub> nanocomposite ( $6.4 \text{ A m}^{-1} \text{ cm}^{-2}$ ) is higher than that of the biosensor based on GMC ( $5.0 \text{ A m}^{-1} \text{ cm}^{-2}$ ) or Co<sub>3</sub>O<sub>4</sub> ( $3.5 \text{ A m}^{-1} \text{ cm}^{-2}$ ), which can be attributed to the synergistic effect of the GMC/Co<sub>3</sub>O<sub>4</sub> nano-

composite. The biosensor is further used to systematically detect mixed phenolic samples (phenol, catechol, *m*-cresol, *p*-cresol, and 4-chlorophenol) and real water samples. The biosensor-based detection results for river water and tap water samples show outstanding average recovery (92.2–103.3%) and relative standard deviations (0.9–7.8%). In comparison with the conventional spectrophotometric method, the biosensor method is more rapid, sensitive, accurate, and convenient. Furthermore, the detection limit of the biosensor method is about 20 times lower than that of the spectrophotometric method. This novel biosensor is proven to be a promising alternative tool for the rapid and on-site monitoring of environmental phenolic pollutants.

## 1. Introduction

Phenolic compounds are widely used in many chemical industries for the production of pesticides, plastics, herbicides, pharmaceuticals, and synthetic products. Owing to their high toxicity and serious threat to human health, the identification and detection of phenolic compounds are of great importance in environmental monitoring.<sup>[1]</sup> Many analytical methods are available for the detection of phenolic compounds, such as spectrophotometry,<sup>[2]</sup> capillary zone electrophoresis,<sup>[3]</sup> high-performance liquid chromatography,<sup>[4]</sup> and liquid chromatography-mass spectrometry.<sup>[5]</sup> However, these methods have inherent disadvantages and limitations including the requirement for highly trained technicians, time-consuming sample preparation, and expensive equipment. Therefore, there is an urgent demand to develop a simple, rapid, cost-effective, and portable device for the determination of phenolic compounds in aqueous environmental samples. The electrochemical tyrosinase (Tyr) biosensor method can be employed to solve the above problems. Without complicated sample pretreatment, the electrochemical Tyr biosensor shows rapid response to phenolic compounds, so it is especially appropriate for the on-site detection of such pollutants. It has been proven to be a highly promising method for the detection of phenolic compounds.<sup>[6]</sup>

The effective immobilization of enzymes is a key factor in the performance of the electrochemical enzyme biosensor. To seek better immobilization approaches, various enzyme immobilization methods have been attempted, such as adsorption, covalent bonding, cross-linking, and entrapment. All of these methods inevitably suffer from problems such as 1) the leakage of immobilized enzyme, 2) low electron-transfer efficiency between the enzyme and the electrode surface, and 3) lack of long-term storage stability.<sup>[7]</sup> To overcome the above problems, various nanomaterials as enzyme-support materials have attracted increasing interest over the past decade. Many kinds of nanomaterials have been developed, such as metal nanoparticles,<sup>[8]</sup> graphene,<sup>[9]</sup> carbon nanotubes,<sup>[10]</sup> carbon nanofibers,<sup>[11]</sup> metal oxides,<sup>[12]</sup> and conducting polymers.<sup>[13]</sup> These materials exhibit high surface area, outstanding electronic-conduction ability, and good biocompatibility for enhancing the performance of electrochemical biosensors.<sup>[14]</sup>


In recent years, graphitized ordered mesoporous carbon (GMC) as a novel carbon-based nanomaterial has received significant interest owing to its extremely well-ordered mesopore structure, high specific surface area, high specific pore volume, and tunable pore diameters, all of which make it attractive for

[a] X. Wang,<sup>+</sup> Prof. X. Lu,<sup>+</sup> Dr. L. Wu, Prof. J. Chen  
Dalian Institute of Chemical Physics, Chinese Academy of Sciences  
No. 457 Zhongshan Road, Dalian 116023 (P.R. China)  
E-mail: xianbolu@dicp.ac.cn  
chenjp@dicp.ac.cn

[b] X. Wang<sup>+</sup>  
University of Chinese Academy of Sciences  
No. 19A Yuquan Road, Beijing 100049 (P.R. China)

[c] Dr. L. Wu  
Chinese Academy of Fishery Sciences  
No. 150 Yongding Road, Beijing 100141 (P.R. China)

[<sup>+</sup>] These authors contributed equally to this work

 Supporting Information for this article is available on the WWW under <http://dx.doi.org/10.1002/cphc.201300208>.

the fabrication of electrochemical biosensors.<sup>[15]</sup> Our previous studies revealed that GMC with proper pore-size matching for enzyme molecules could accommodate enzyme molecules into their mesopores thus to provide a protective microenvironment to prevent enzyme deactivation.<sup>[16]</sup> Some successful applications were reported on enzyme molecules immobilized on GMC for the fabrication of biosensors.<sup>[17]</sup> However, nanocomposites made from the assembly of GMC and a nanostructured metal oxide have been rarely explored for the fabrication of biosensors. Kim et al. developed a conductive mult catalyst system consisting of  $\text{Fe}_3\text{O}_4$  magnetic nanoparticles and oxidative enzymes co-entrapped in the pores of mesoporous carbon, and the performance of this electrochemical glucose biosensor was significantly improved.<sup>[18]</sup> Nanostructured metal oxides can provide highly effective surfaces for enzyme immobilization and the prospect of improving the performance of the biosensor by way of promoting faster electron transfer between the active site of the desired enzyme and the electrode surface is excellent. In our previous work, hemoglobin was entrapped within layered spongy  $\text{Co}_3\text{O}_4$  to fabricate a hydrogen peroxide biosensor. The biosensor showed excellent bioelectrocatalytic activity towards  $\text{H}_2\text{O}_2$  due to the introduction of the  $\text{Co}_3\text{O}_4$  nanosheet.<sup>[19]</sup> In this paper, we will make use of a nanocomposite based on mesoporous carbon and  $\text{Co}_3\text{O}_4$  nanorods to fabricate an electrochemical Tyr biosensor for the detection of phenolic compounds. Unlike single nanomaterials, nanocomposites can take advantage of the synergistic effect of the different nanomaterials to exhibit better biosensing performance.

Real environmental samples consist of complicated components including various phenolic compounds, such as phenol, cresol, and chlorophenol. In previous studies, Tyr biosensors were usually developed for the detection of a specific kind of phenolic compound,<sup>[6,20]</sup> and biosensors for detecting mixed phenolic compounds were rarely reported. Herein, in the present study and on the basis of the amperometric response of the biosensor for single phenolic samples, a rapid detection method for mixed phenolic samples and real environmental samples is developed. In comparison with conventional spectrophotometric methods, the greatest advantage of the biosensor method is that it does not need complicated and time-consuming sample pretreatment, and the detection results are closer to the true values. This biosensor method could meet the demand for the rapid and on-site detection of phenolic pollutants in real environmental samples.

## 2. Results and Discussion

### 2.1. Morphological and Electrochemical Impedance Spectroscopy Characterization of GMC/ $\text{Co}_3\text{O}_4$ -Tyr-Chitosan Nanocomposite

The morphology of the GMC,  $\text{Co}_3\text{O}_4$  nanorods, and GMC/ $\text{Co}_3\text{O}_4$  nanocomposite is shown in the transmission electron microscopy (TEM) images, which can be seen in Figure 1. GMC with a good pore-size matching for Tyr molecules ( $6.5 \times 9.8 \times 5.5 \text{ nm}^3$ ) was synthesized by using 10 nm silica nanospheres as

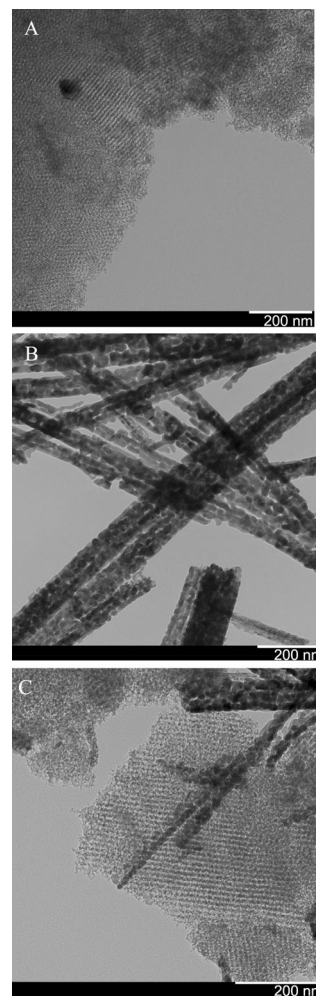


**Figure 1.** TEM images of A) GMC (pore diameter 10 nm), B)  $\text{Co}_3\text{O}_4$  nanorods, and C) GMC/ $\text{Co}_3\text{O}_4$  nanocomposite.

a template. As shown, GMC exhibits a highly ordered porous structure with a pore diameter of 10 nm, which is indicative of the formation of an ordered mesoporous structure. These spherical pores are interconnected by adjacent smaller windows, which could provide mass-transfer channels for the enzyme-catalyzed substrate and product.<sup>[21]</sup> More importantly, the mesopores with a pore size of 10 nm could provide a favorable microenvironment to accommodate the Tyr molecules. Figure 1 b clearly displays the morphology of uniform nanorod-shaped  $\text{Co}_3\text{O}_4$ . The  $\text{Co}_3\text{O}_4$  nanorods are around 100 nm in diameter and several micrometers in length. The morphology is considered as an important characteristic of one-dimensional nanostructures, which is a key factor that affects the ultimate electrochemical performance.  $\text{Co}_3\text{O}_4$  nanorods are a promising nanomaterial for electrochemical devices due to their excellent electrochemical properties.<sup>[22]</sup> The GMC/ $\text{Co}_3\text{O}_4$  nanocomposite was obtained by vibrating GMC with  $\text{Co}_3\text{O}_4$  nanorods together under sonication conditions for 0.5 h. As shown in Figure 1 c, the  $\text{Co}_3\text{O}_4$  nanorods are distributed on the surface of GMC so as to form the GMC/ $\text{Co}_3\text{O}_4$  nanocomposite. Our previous study revealed that GMC with proper pore-size matching for enzyme molecules could accommodate enzyme molecules into their

mesopores thus to provide a protective microenvironment to prevent enzyme deactivation.<sup>[16,21]</sup> As for  $\text{Co}_3\text{O}_4$ , it has good hydrophilicity and biocompatibility.<sup>[19]</sup> The combination of  $\text{Co}_3\text{O}_4$  with GMC resulted in the formation of a novel nanocomposite with improved hydrophilicity and biocompatibility. The synergistic effect of the nanocomposite is believed to play a positive role in the electron transfer between the redox enzyme and the electrode surface.

Electrochemical impedance spectroscopy (EIS) was used to characterize the interface properties of the GMC/ $\text{Co}_3\text{O}_4$ -Tyr-Chi (in which Chi = chitosan) nanocomposite-modified electrodes. In EIS, the semicircle portion observed at high frequencies corresponds to the electron-transfer ability.<sup>[23]</sup> The charge-transfer resistance ( $R_{\text{ct}}$ ), which controls the electron-transfer kinetics of the redox probe at the electrode interface, can be gained by measuring the diameter of the semicircle. Figure 2 shows the Nyquist plots of bare glassy carbon electrode (GCE), Tyr-Chi/GCE,  $\text{Co}_3\text{O}_4$ -Tyr-Chi/GCE, GMC-Tyr-Chi/GCE, and GMC/ $\text{Co}_3\text{O}_4$ -Tyr-

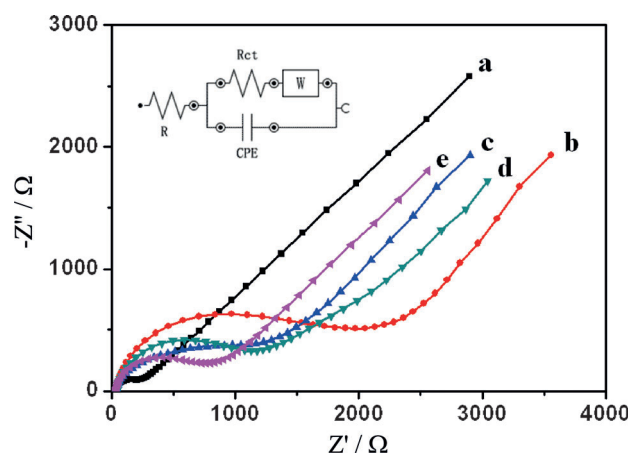


**Figure 2.** Alternating-current impedance spectra of bare GCE (a), Tyr-Chi/GCE (b),  $\text{Co}_3\text{O}_4$ -Tyr-Chi/GCE (c), GMC-Tyr-Chi/GCE (d), and GMC/ $\text{Co}_3\text{O}_4$ -Tyr-Chi/GCE (e) in 1.0 mM  $\text{Fe}(\text{CN})_6^{3-/4-}$  containing 0.5 M  $\text{KNO}_3$  solution. The frequency range was from  $1 \times 10^5$  to  $1 \times 10^{-1}$  Hz. Inset: Randles equivalent circuit used to fit the experimental data.

Chi/GCE obtained in a 1.0 mM  $\text{Fe}(\text{CN})_6^{3-/4-}$  solution containing 0.5 M  $\text{KNO}_3$ . After fitting the data, the values of  $R_{\text{ct}}$  for different electrodes were obtained in the following order: Tyr-Chi/GCE (1.7 k $\Omega$ ) >  $\text{Co}_3\text{O}_4$ -Tyr-Chi/GCE (1.1 k $\Omega$ ) > GMC-Tyr-Chi/GCE (1.0 k $\Omega$ ) > GMC/ $\text{Co}_3\text{O}_4$ -Tyr-Chi/GCE (0.7 k $\Omega$ ) > bare GCE (181  $\Omega$ ). As can be observed, bare GCE (Figure 2, curve a) presents a small semicircle domain, which implies that it is almost a diffusion-limiting process. After casting a layer of different nanocomposites, large semicircles at high frequencies were obtained, and this indicates that the electron transfer of the redox probe was obstructed. The  $R_{\text{ct}}$  of Tyr-Chi/GCE (Figure 2, curve b) was the largest; this demonstrates that the Chi film and Tyr molecules hindered the electron transfer. With  $\text{Co}_3\text{O}_4$  or GMC modified on Tyr-Chi/GCE, the semicircle clearly decreased (Figure 2, curves c, d). The reason for the lower charge-transfer resistance is probably because the  $\text{Co}_3\text{O}_4$  or GMC nanomaterial could form high electron-conduction pathways

to dramatically enhance the electron-transfer ability of the enzyme electrode. Notably, the value of  $R_{\text{ct}}$  for GMC/ $\text{Co}_3\text{O}_4$ -Tyr-Chi/GCE (Figure 2, curve e) further decreased significantly, which is the best electrochemical behavior among the studied electrodes. This suggests that the GMC/ $\text{Co}_3\text{O}_4$  nanocomposite could make the electron transfer from the enzyme electrode easier and provide a sufficient number of available conducting sites to allow the electrochemical reaction to be performed.

## 2.2. Direct Electrochemistry of GMC/ $\text{Co}_3\text{O}_4$ -Tyr-Chi/GCE

Great efforts have been made to achieve direct electrochemistry of Tyr, as it can be used to fabricate third-generation biosensors (requiring no mediator) with good analytical performance.<sup>[20,24]</sup> However, very few studies have reported the efficient direct electron transfer between Tyr and the electrode, as the electroactive center of Tyr is deeply embedded in the enzyme molecule. In this regard, we used the GMC/ $\text{Co}_3\text{O}_4$  nanocomposite as an enzyme immobilization matrix to achieve the direct electrochemistry of Tyr. To study the direct electron transfer of Tyr immobilized on the GMC/ $\text{Co}_3\text{O}_4$  nanocomposite, cyclic voltammetry (CV) measurements were performed in 50 mM  $\text{N}_2$ -saturated phosphate buffer saline (PBS, pH 7.0) at a scan rate of 100  $\text{mVs}^{-1}$ . In our study, 50 mM pH 7.0 PBS was used as the electrolyte in the electrochemical experiments because Tyr has the highest bioactivity in this pH value. No clear redox peak was observed at Tyr-Chi/GCE (Figure 3a, curve c) or GMC/ $\text{Co}_3\text{O}_4$ -Chi/GCE (figure not shown). In contrast, a pair of well-defined redox peaks was observed on GMC-Tyr-Chi/GCE (Figure 3a, curve b). This difference resulted from the fact that GMC could significantly enhance the direct electron transfer between the Tyr molecules and the GCE. First, the large surface area and excellent electronic conductivity of GMC provided a large number of favorable sites for electron transfer. Second, the pore size (pore diameter of 10 nm) of GMC matched the size of the Tyr molecules ( $6.5 \times 9.8 \times 5.5$  nm), so GMC could provide a protective microenvironment for the immobilized proteins to prevent inactivation.<sup>[16,21]</sup> With the addition of  $\text{Co}_3\text{O}_4$  nanorods, a pair of more distinct redox peaks was observed on GMC/ $\text{Co}_3\text{O}_4$ -Tyr-Chi/GCE (Figure 3a, curve a), which indicated that more Tyr molecules on GMC/ $\text{Co}_3\text{O}_4$ -Tyr-Chi/GCE could participate in direct electron transfer between the active center of the Tyr molecule and the electrode. Nanostructured metal oxides can provide a biocompatible electroactive surface for enzyme immobilization.<sup>[25]</sup> With the addition of the  $\text{Co}_3\text{O}_4$  nanorods, more Tyr molecules on GMC/ $\text{Co}_3\text{O}_4$ -Tyr-Chi/GCE could participate in direct electron transfer between the active center of the Tyr molecules and the electrode. Clearly, the  $\text{Co}_3\text{O}_4$  nanorods played a synergistic role with GMC in facilitating the direct electron transfer of Tyr.

Figure 3b shows the CV curves of the GMC/ $\text{Co}_3\text{O}_4$ -Tyr-Chi/GCE biosensor recorded in PBS (50 mM, pH 7.0) at different scan rates from 10 to 100  $\text{mVs}^{-1}$ . Both the anodic peak current ( $I_{\text{pa}}$ ) and the cathodic peak current ( $I_{\text{pc}}$ ) increased linearly with an increase in the scan rate. This revealed that the electron transfer between Tyr and the GCE was a surface-controlled process.<sup>[26]</sup> If  $n\Delta E_p < 200$  mV (in which  $n$  is the number of trans-

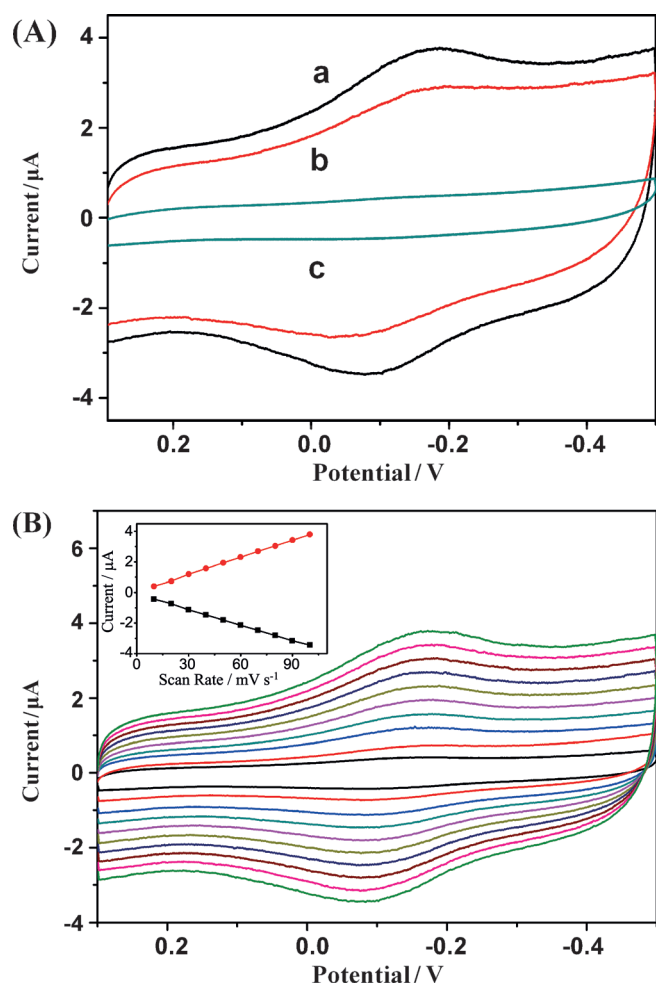


**Figure 3.** A) CV curves of GMC/Co<sub>3</sub>O<sub>4</sub>-Tyr-Chi/GCE (a), GMC-Tyr-Chi/GCE (b), and Tyr-Chi/GCE (c) in N<sub>2</sub>-saturated 50 mM pH 7.0 PBS at a scan rate of 100 mV s<sup>-1</sup>. B) CV curves of GMC/Co<sub>3</sub>O<sub>4</sub>-Tyr-Chi/GCE in 50 mM pH 7.0 PBS buffer at scan rates of 10, 20, 30, 40, 50, 60, 70, 80, 90, and 100 mV s<sup>-1</sup> (from inner to outer). Inset: Plot of cathodic and anodic peak currents versus scan rates.

ferred electrons and  $\Delta E_p$  is the peak separation between anodic and cathodic peaks), the electron-transfer rate constant ( $k_s$ ) was estimated to be 1.16 s<sup>-1</sup> according to the Laviron method<sup>[27]</sup> [Eq. (1)]:

$$k_s = mnFv/RT \quad (1)$$

in which  $m$  is a parameter related to the peak-to-peak separation,  $n$  is the number of transferred electrons,  $F$  is the Faraday constant,  $R$  is the universal gas constant,  $T$  is the temperature, and  $v$  is the scan rate.

The value of  $k_s$  is much higher than  $k_s = 0.032$  s<sup>-1</sup> for Tyr adsorbed on gold nanoparticle modified boron-doped diamond electrode<sup>[20]</sup> and much higher than  $k_s = 0.9$  s<sup>-1</sup> for Tyr covalently bound to a glassy carbon electrode through Woodward's reagent K.<sup>[24a]</sup> These results suggest that the combination of GMC and Co<sub>3</sub>O<sub>4</sub> nanorods resulted in a faster electron-transfer process.

### 2.3. Bioelectrocatalytic Activity of GMC/Co<sub>3</sub>O<sub>4</sub>-Tyr-Chi/GCE towards Catechol

To evaluate the bioelectrocatalytic activity of GMC/Co<sub>3</sub>O<sub>4</sub>-Tyr-Chi/GCE, the modified electrode was characterized by CV in the presence of catechol in the potential range between +0.3 and -0.5 V. Figure S1 (Supporting Information) shows the cyclic voltammograms of GMC/Co<sub>3</sub>O<sub>4</sub>-Tyr-Chi/GCE in 50 mM PBS (pH 7.0) in the presence of 10  $\mu$ M catechol (Figure S1, curve a) and in the absence of catechol (Figure S1, curve b) at a scan rate of 100 mV s<sup>-1</sup>. It was observed that with the addition of 10  $\mu$ M catechol, both the oxidation current and reduction current increased. Clearly, the observed increase in the redox current was attributed to the enzyme-catalyzed reaction on the electrode surface. The major steps in the enzymatic reaction are shown in Equations (2) and (3):<sup>[6b]</sup>



At a relatively low potential (-0.1 V peak potential), a larger response toward catechol was observed. Notably, a relatively low applied potential was most important for the Tyr-based biosensor, as it reduced possible interferences in the detection. Thus, for further amperometric study of GMC/Co<sub>3</sub>O<sub>4</sub>-Tyr-Chi/GCE, a potential of -0.1 V (vs. Ag/AgCl, 3 M KCl) was applied.

### 2.4. Amperometric Biosensing of Phenolic Compounds

Amperometry is a more sensitive electroanalytical method for the detection of phenolic compounds than cyclic voltammetry. Figure 4 illustrates the typical current-time plot of the GMC/Co<sub>3</sub>O<sub>4</sub>-Tyr-Chi/GCE biosensor with the successive addition of catechol into stirring 50 mM PBS (8 mL, pH 7.0). The biosensor exhibited a rapid and sensitive response with changes in the

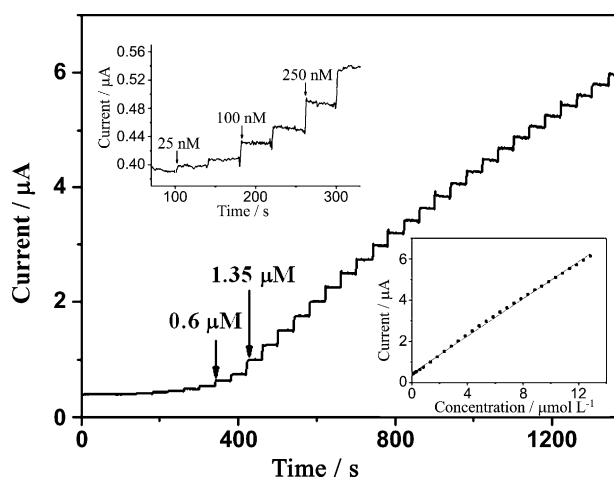


**Figure 4.** Typical amperometric current-time response curves for the GMC/Co<sub>3</sub>O<sub>4</sub>-Tyr-Chi/GCE biosensor upon the sequential addition of catechol with different concentrations into a stirring solution of 50 mM PBS (pH 7.0, 8 mL). Applied potential: -0.1 V versus Ag/AgCl. Upper inset: amplified response curve. Lower inset: linear calibration curve.



catechol concentration and reached about 95% of the steady-state current within 2 s after each addition of catechol. Such a fast response indicated that the analyte molecules achieved rapid diffusion between the electrode surface and the electrolyte solution. The linear range of the biosensor was from  $5.0 \times 10^{-8}$  to  $1.3 \times 10^{-5}$  M with a correlation coefficient of 0.9992 for catechol. The detection limit was estimated to be 25 nM at a signal-to-noise ratio of 3. The analytical performance of the GMC/Co<sub>3</sub>O<sub>4</sub>-Tyr-Chi/GCE biosensor was compared with that of other Tyr biosensors reported in the literature. From Table 1, we can see that the developed GMC/Co<sub>3</sub>O<sub>4</sub>-Tyr-Chi/GCE biosensor exhibited improved analytical performance in terms of the limit of detection and the response time in comparison with other reported biosensors for which different materials were used as the immobilization matrix. This result indicated that our developed biosensor was an excellent candidate for the detection of phenolic compounds. The sensitivity of the GMC/Co<sub>3</sub>O<sub>4</sub>-Tyr-Chi/GCE biosensor ( $6.4 \text{ A M}^{-1} \text{ cm}^{-2}$ ) was higher than that of the GMC-Tyr-Chi/GCE biosensor ( $5.0 \text{ A M}^{-1} \text{ cm}^{-2}$ ), the Co<sub>3</sub>O<sub>4</sub>-Tyr-Chi/GCE biosensor ( $3.5 \text{ A M}^{-1} \text{ cm}^{-2}$ ), and the Tyr-Chi/GCE biosensor ( $3.0 \text{ A M}^{-1} \text{ cm}^{-2}$ ) (Figure 5). The higher sensitivity of GMC/Co<sub>3</sub>O<sub>4</sub>-Tyr-Chi/GCE could be attributed to the synergistic effect of the GMC/Co<sub>3</sub>O<sub>4</sub> nanocomposite, which dramatically enhanced the direct electron transfer and the bioelectrocatalytic activity of the enzyme electrode.

The GMC/Co<sub>3</sub>O<sub>4</sub>-Tyr-Chi/GCE biosensor exhibited a highly sensitive response to phenolic compounds, such as catechol, phenol, *p*-cresol, *m*-cresol, and 4-chlorophenol. The detection results including the linear range, correlation coefficient, sensitivity, detection limit, and apparent Michaelis–Menten constant ( $K_m^{\text{app}}$ ) are summarized in Table 2. From Table 2, it was found that the sensitivity of the developed biosensor follows the order: catechol > *p*-cresol > 4-chlorophenol > phenol > *m*-cresol, ranging from 6.4 to  $3.4 \text{ A M}^{-1} \text{ cm}^{-2}$ . The apparent Michaelis–Menten constant as a parameter of enzyme–substrate kinetics is a reflection of enzymatic affinity. According to the Lineweaver–Burk equation [Eq. (4)],<sup>[36]</sup> the  $K_m^{\text{app}}$  values were 21.5, 20.2, 15.9, 12.3, and  $14.2 \mu\text{M}$  for catechol, phenol, *p*-cresol, *m*-cresol, and 4-chlorophenol, respectively. Such low values showed that the GMC/Co<sub>3</sub>O<sub>4</sub> nanocomposite modified Tyr biosensor had good enzymatic activity and high affinity for phenolic compound sub-

**Table 1.** Comparison of the analytical performance of the GMC/Co<sub>3</sub>O<sub>4</sub>-Tyr-Chi/GCE biosensor with that of other Tyr biosensors.

Modified electrode <sup>[a]</sup>	Linear range [ $\mu\text{M}$ ]	Sensitivity	Detection limit [ $\mu\text{M}$ ]	Response time [s]	Ref.
Au/PASE-GO-Tyr	0.083–23	$0.16 \text{ A M}^{-1}$	0.024	6	[6b]
Ppy-Tyr	1–16	$10 \text{ mV } \mu\text{M}^{-1}$	1	80	[28]
thionine-Tyr	0.15–75	$0.1396 \pm 0.0011 \text{ A M}^{-1}$	0.15	100	[29]
polyamidic nanofibrous membrane-Tyr	1–100	$0.304 \text{ A M}^{-1}$	0.050	16	[30]
PO <sub>4</sub> -Ppy-Tyr	10–120	$0.047 \text{ A M}^{-1}$	0.84	5	[31]
HTLc-Tyr	3–300	–	0.1	–	[32]
MWCNT-DTDAB-Tyr	2–15	$3.100 \text{ A M}^{-1}$	0.9	–	[33]
AuNPs-MPTS-Tyr	1.7–96	$0.3067 \text{ A M}^{-1} \text{ cm}^{-2}$	0.56	8	[34]
sol-gel-AuNPs-Tyr	1–60	$0.01 \text{ A M}^{-1}$	0.3	–	[35]
GMC/Co <sub>3</sub> O <sub>4</sub> -Tyr-Chi	0.05–13	$6.4 \text{ A M}^{-1} \text{ cm}^{-2}$	0.025	2	this paper

[a] PASE = pyrenebutanoic acid succinimidyl ester, GO = graphene oxide, Ppy = polypyrrole, HTLc = Mg–Al–CO<sub>3</sub> hydrotalcite-like compound, MWCNT = multiwall carbon nanotube, DTDAB = dimethylditetradecylammonium bromide, AuNPs = gold nanoparticles, MPTS = (3-mercaptopropyl)-trimethoxysilane.

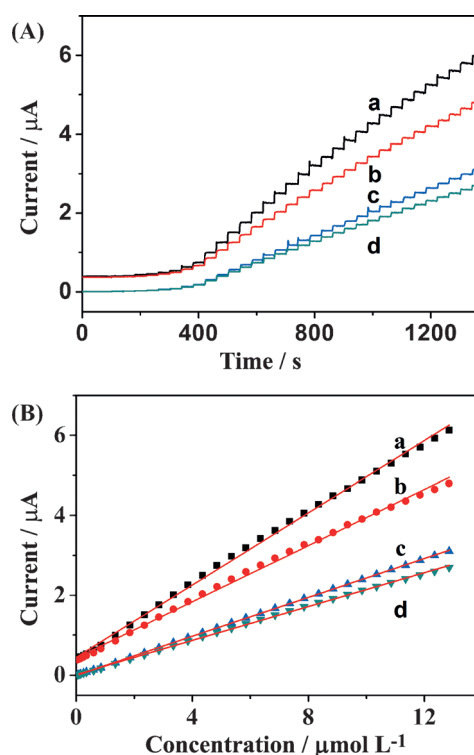


**Figure 5.** A) The amperometric current response curves of the GMC/Co<sub>3</sub>O<sub>4</sub>-Tyr-Chi/GCE biosensor (a), GMC-Tyr-Chi/GCE biosensor (b), Co<sub>3</sub>O<sub>4</sub>-Tyr-Chi/GCE biosensor (c), and Tyr-Chi/GCE biosensor (d) with the sequential addition of catechol into a stirring solution of 50 mM PBS (pH 7.0, 8 mL). Applied potential:  $-0.1 \text{ V}$  versus Ag/AgCl. B) Linear calibration curves obtained at the four kinds of biosensors.

**Table 2.** Response characteristics of the GMC/Co<sub>3</sub>O<sub>4</sub>-Tyr-Chi/GCE biosensor to phenolic compounds.

Phenolic compound	Linear range [M]	Correlation coefficient	Sensitivity [ $\text{A M}^{-1} \text{ cm}^{-2}$ ]	Detection limit [nM]	$K_m^{\text{app}}$ [ $\mu\text{M}$ ]
catechol	$5.0 \times 10^{-8}$ – $1.3 \times 10^{-5}$	0.9992	6.4	25	21.5
phenol	$5.0 \times 10^{-8}$ – $1.1 \times 10^{-5}$	0.9994	5.1	25	20.2
<i>p</i> -cresol	$3.5 \times 10^{-7}$ – $9.8 \times 10^{-6}$	0.9985	6.1	100	15.9
<i>m</i> -cresol	$1.3 \times 10^{-7}$ – $1.0 \times 10^{-5}$	0.9991	3.4	50	12.3
4-chlorophenol	$3.8 \times 10^{-7}$ – $1.0 \times 10^{-6}$	0.9981	5.8	125	14.2

strates. These results indicated that the Tyr biosensor had a prominent ability to detect a wide variety of phenolic compounds. The GMC/Co<sub>3</sub>O<sub>4</sub>-Tyr-Chi/GCE biosensor exhibited little difference regarding sensitivity, limit of detection, and  $K_m^{app}$  for the different volatile phenolic chemicals, and this indicates that it can be used as a powerful tool for the detection and evaluation of mixed volatile phenolic compounds in samples.

$$\frac{1}{I_{ss}} = \frac{K_m^{app}}{I_{max}} \frac{1}{[S]} + \frac{1}{I_{max}} \quad (4)$$

in which  $I_{ss}$  is the steady-state current after the addition of the substrate,  $I_{max}$  is the maximum current measured under the saturated substrate conditions, and  $[S]$  is the concentration of the substrate.

## 2.5. The Detection of Mixed Phenolic Compounds

In previous studies, some Tyr biosensors were developed for the detection of a specific kind of phenolic compound, and biosensors for detecting mixed phenolic compounds have been rarely reported. In practical application, real samples usually consist of mixed phenolic pollutants. To investigate the amperometric response characteristic for mixed phenolic samples, the Tyr biosensor was used to detect a mixed phenolic solution composed of catechol, phenol, *p*-cresol, *m*-cresol, and 4-chlorophenol all at the same concentration. The spectrophotometric method is the national standard method of China and many other countries for detecting phenolic compounds, but its sample pretreatment is complicated and time consuming. In the following, we compared the detection results of the biosensor with those of the 4-aminoantipyrine spectrophotometric method environment protection standard HJ 503-2009 of the People's Republic of China). The mixed phenolic samples (total concentrations: 20, 40, 60, and 80  $\mu\text{M}$ ) were first tested by the 4-aminoantipyrine spectrophotometric method. Then, the above samples were tested by the biosensor after a 20-fold dilution (because the sensitivity of the fabricated biosensor was much higher than that of the spectrophotometric method). The detection results obtained by both UV/Vis and the biosensor were converted into phenol-equivalent concentrations, and the relevance between them is shown in Figure 6. According to the experimental results, there was a good positive correlation between the detection results of the biosensor and those of the spectrophotometric method. However, the biosensor was much more sensitive than spectrophotometry for the detection of mixed phenolic chemicals, and the detection limit of the biosensor was about 20 times lower than that of the spectrophotometric method. Furthermore, as shown in Figure 6a, the detection results of the biosensor were clearly closer to the true values of the real samples. Compared with the spectrophotometric and chromatographic methods, the greatest advantage of the biosensor method was that it did not need a complicated and time-consuming sample pretreatment process, and the whole detection process could be completed within several minutes. This biosensor method proved

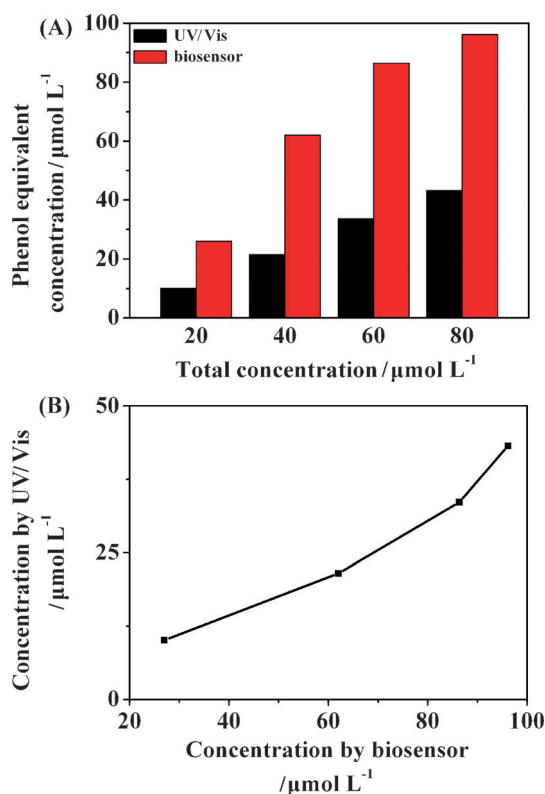


**Figure 6.** A) Phenol equivalent concentration determined by the GMC/Co<sub>3</sub>O<sub>4</sub>-Tyr-Chi/GCE biosensor method and the 4-aminoantipyrine spectrophotometric method for mixed phenolic compounds. B) Comparison of the determined concentrations of mixed phenolic compounds by the biosensor and 4-aminoantipyrine spectrophotometric methods.

to be a powerful alternative to these available analytical methods and has potential application for the rapid and on-site determination of total phenolic content in environmental samples.

## 2.6. Selectivity, Stability, Repeatability, and Real Sample Analysis

The selectivity of the biosensor was investigated by detecting the amperometric response to some possible interferents in the presence of 2  $\mu\text{M}$  catechol. The results showed that the response was not affected by 40  $\mu\text{M}$  uric acid, 2 mM glucose, and 0.1 mM H<sub>2</sub>O<sub>2</sub> (Figure S2). Moreover, inorganic ions (2 mM K<sup>+</sup>, Na<sup>+</sup>, NO<sub>3</sub><sup>-</sup>, H<sub>2</sub>PO<sub>4</sub><sup>-</sup>, HPO<sub>4</sub><sup>2-</sup>, Cl<sup>-</sup>, and Ac<sup>-</sup>) and organic solvents (0.25 % v/v acetone, acetonitrile, methanol, and ethanol) also had no influence on the performance of the biosensor (data not shown). Long-term storage stability is of great importance to its application in environmental monitoring. The storage stability of the biosensor was evaluated by detecting the amperometric response to 1  $\mu\text{M}$  catechol. The activity of the biosensor was 86% after 2 months in PBS (50 mM, pH 7.0) at 4 °C; this is indicative of excellent long-term storage stability. The repeatability of the biosensor was investigated by detecting the amperometric responses to 0.5  $\mu\text{M}$  catechol over ten successive additions. The relative standard deviation (RSD) was

6.1%, which demonstrates the good repeatability of the method.

To further demonstrate the practicality of the biosensor, it was used to detect real environmental water samples. The recovery test was studied by adding spiked catechol into tap water and river water. River water samples were collected from the Xiaobei River (Liaoyang city, Liaoning) in June 2013. Water samples were transported to the laboratory and were stored at 4 °C in glass containers before analysis. Tap water samples were taken from our laboratory in the Shahekou district, Dalian. All samples were filtered through a 0.22 µm filter membrane before use to remove suspended solids. The results are summarized in Table 3. If the concentration of catechol was in the 0.2 to 5.0 µM range, the recovery was 93.2–102.7% and the RSD was 1.7–7.8% in tap water; the recovery was 92.2–103.3% and the RSD was 0.9–7.1% in river water. The results confirmed that the fabricated biosensor was applicable for the practical detection of phenolic pollutants.

**Table 3.** Recovery of the GMC/Co<sub>3</sub>O<sub>4</sub>-Tyr-Chi/GCE biosensor.

Sample	Catechol added [µM]	Found <sup>[a]</sup> [µM]	Recovery [%]	RSD [%]
tap water	0.2	0.202	101.0	1.7
	0.5	0.481	96.2	6.4
	1.0	0.932	93.2	4.9
	2.0	1.928	96.4	3.2
	3.0	3.081	102.7	4.7
	5.0	4.725	94.5	7.8
river water	0.2	0.201	100.5	3.9
	0.5	0.515	103.0	0.9
	1.0	1.033	103.3	1.5
	2.0	2.040	102.0	2.2
	3.0	3.051	101.7	7.1
	5.0	4.610	92.2	6.6

[a] The average value of three determinations.

### 3. Conclusions

In this paper, an electrochemical Tyr biosensor based on a nanostructured GMC/Co<sub>3</sub>O<sub>4</sub> nanocomposite was constructed for the detection of phenolic compounds. The synergistic effects of the GMC/Co<sub>3</sub>O<sub>4</sub> nanocomposite dramatically facilitated direct electron transfer. In comparison with GMC or Co<sub>3</sub>O<sub>4</sub> alone, the nanocomposite significantly improved the sensitivity of the Tyr biosensor. Compared with the spectrophotometric and chromatographic method, the greatest advantage of the biosensor method was that it did not need complicated and time-consuming sample pretreatment processes. The detection limit of the biosensor was about 20 times lower than that of the spectrophotometric method, and the detection results of the biosensor were closer to the true values in the mixed phenolic samples. The biosensor was further used for the detection of phenolic compounds in tap water and river water and good average recovery and RSDs were achieved, which indicated that the biosensor was a reliable tool for real samples. The fabricated biosensor displayed good selectivity and long-term

stability. The GMC/Co<sub>3</sub>O<sub>4</sub> nanocomposite provided a robust, efficient, and universal electrochemical biosensing platform for the fabrication of various enzyme biosensors. The Tyr biosensor based on the GMC/Co<sub>3</sub>O<sub>4</sub> nanocomposite proved to be a great potential device for the rapid and on-site monitoring of phenolic pollutants in environmental samples.

## Experimental Section

### Material and Methods

Chi (from crab shells, minimum 85% deacetylated) and Tyr (from mushroom, >1000 units mg<sup>-1</sup>) were purchased from Sigma. All other reagents were of analytical grade and were used as received without further purification. Phosphate buffer saline (PBS, 50 mM, pH 7.0) was prepared by mixing standard solutions of K<sub>2</sub>HPO<sub>4</sub> and KH<sub>2</sub>PO<sub>4</sub>. Milli-Q water (18.2 MΩ cm) was used for the preparation of PBS.

Transmission electron microscopy (TEM) images were obtained with a Hitachi HT7700 (Hitachi, Japan) microscope with an accelerating voltage of 120 kV. UV/Vis tests were performed with a SP-1901 spectrophotometer (Spectrum Shanghai, China). Electrochemical impedance spectroscopy (EIS) measurements were performed with an Autolab potentiostat PGSTAT302N (Eco Chemie, The Netherlands). Cyclic voltammetry (CV) and amperometric measurements were performed with a CHI 440A Electrochemical Workstation (Chenhua Instruments, China). All measurements were based on a three-electrode system with the prepared enzyme electrode as the working electrode, a Ag/AgCl electrode (KCl concentration: 3 M) as the reference electrode, and a platinum wire as the auxiliary electrode.

### Preparation of GMC, Co<sub>3</sub>O<sub>4</sub>, and the GMC/Co<sub>3</sub>O<sub>4</sub> Nanocomposite

The graphitized ordered mesoporous carbon was prepared by a template-assisted method according to our previously reported method.<sup>[21]</sup> Briefly, monodisperse silica nanospheres (10 nm) were synthesized through the Stöber method reported by Yokoi with minor revision.<sup>[37]</sup> The final mass composition of tetraethoxysilane, L-lysine, and H<sub>2</sub>O in the solution was 1:0.01:78. The above mixed solution was stirred for 12 h at 70 °C, followed by direct evaporation of the solvent at 80 °C. The obtained silica was calcined in a muffle furnace at 600 °C to remove L-lysine. Then, the GMC with a pore size of 10 nm was synthesized by using the obtained 10 nm silica nanospheres as a template according to our previously reported procedure.<sup>[16]</sup> Briefly, dried silica spheres (1.0 g) were impregnated with 0.5 mm Ni(NO<sub>3</sub>)<sub>2</sub>·6H<sub>2</sub>O aqueous solution (the volume ratio of ethanol/water was 1) and then dried at 45 °C. After grinding in an agate mortar, these silica particles were pressed into pellets at a pressure of 3 × 10<sup>3</sup> kPa to create the silica template. Then, the silica template sheets were immersed into the preliminarily polymerized polystyrene solution (by adding 0.15 mL H<sub>2</sub>SO<sub>4</sub> into 10 mL styrene monomer under vigorous stirring), followed by heating the composite at 160 °C for 24 h to allow the impregnation of polystyrene into the interstices of the silica template. Thereafter, the composite was pyrolyzed/carbonized at 950 °C for 3 h under an argon atmosphere and then cooled to room temperature. The silica template was removed from the composite by using 20% HF over 24 h, followed by washing with copious amounts of an HCl aqueous solution, deionized water, and ethanol and drying at 120 °C to yield the final graphitized ordered mesoporous carbons.



The  $\text{Co}_3\text{O}_4$  nanorods were synthesized by a hydrothermal method.<sup>[38]</sup> Briefly, a solution of  $\text{CO}(\text{NH}_2)_2$  (0.05 M in Milli-Q water, 20 mL) was dropwise added to a solution of  $\text{CoCl}_2$  (0.25 M in Milli-Q water, 20 mL) with stirring, and then the mixed solution was sealed in a Teflon-lined autoclave and heated at  $110^\circ\text{C}$  for 6 h. After slow cooling to room temperature, the obtained precipitate was collected, washed, and dried. This precursor was then calcined by heating from room temperature to  $300^\circ\text{C}$  at a rate of  $1^\circ\text{C min}^{-1}$  and maintained at that temperature for 0.5 h.

The GMC/ $\text{Co}_3\text{O}_4$  nanocomposite was obtained by mixing an aliquot of GMC with  $\text{Co}_3\text{O}_4$  together and then vibrating and sonicating their water dispersion (containing  $0.4\text{ mg mL}^{-1}$  GMC and  $1.0\text{ mg mL}^{-1}$   $\text{Co}_3\text{O}_4$ ) for 0.5 h.

### Preparation and Electrochemical Measurements of the Enzyme Electrodes

Prior to modification, a glassy carbon electrode (GCE, 3 mm diameter) was polished carefully on a polishing cloth by sequentially using 1.0, 0.3, and  $0.05\text{ }\mu\text{m}$  alumina powder and then rinsed with Milli-Q water followed by sonication in ethanol and Milli-Q water. Then, the electrode was dried with a purified nitrogen stream. To get the best performance of the biosensor, the composition of GMC/ $\text{Co}_3\text{O}_4$ -Tyr-Chi was optimized. The final composition of GMC,  $\text{Co}_3\text{O}_4$ , Tyr, and Chi was 0.2, 0.5, 2.5, and  $1.5\text{ mg mL}^{-1}$ , respectively. The preparation process is illustrated in Scheme 1: First, a solution of Tyr ( $10\text{ mg mL}^{-1}$ ,  $10\text{ }\mu\text{L}$ ) was added to a suspension of GMC ( $0.8\text{ mg mL}^{-1}$ ,  $10\text{ }\mu\text{L}$ ), and the mixture was shaken for 1 h. Then,

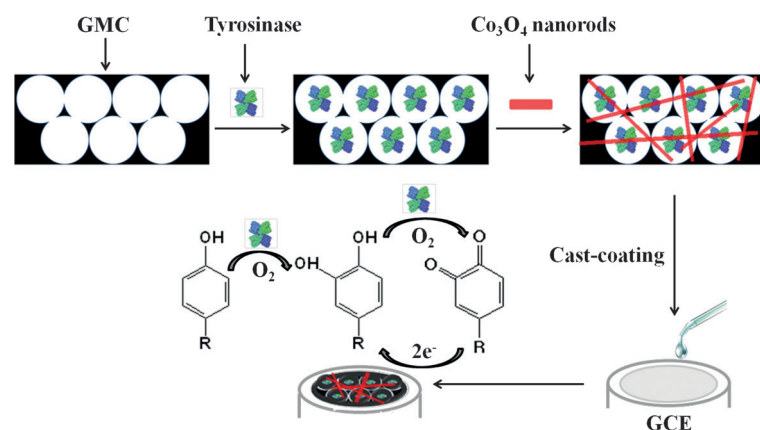
containing Tyr ( $2.5\text{ mg mL}^{-1}$ ) and Chi ( $1.5\text{ mg mL}^{-1}$ ) was used to prepare the Tyr-Chi/GCE biosensor. Before electrochemical measurements, all the Tyr-based electrodes were stirred in 50 mM PBS (pH 7.0) for 30 min to remove residual components.

Cyclic voltammetry measurements were performed in pH 7.0 PBS at a scan rate of  $100\text{ mV s}^{-1}$  ranging from  $+0.3$  to  $-0.5\text{ V}$ . Amperometric measurements were performed in 8 mL stirring pH 7.0 PBS for additions of phenolic compound solutions at an operating potential of  $-0.1\text{ V}$ . EIS measurements were performed in 1 mM  $\text{K}_3[\text{Fe}(\text{CN})_6]/\text{K}_4[\text{Fe}(\text{CN})_6]$  solution containing 0.5 M  $\text{KNO}_3$ , and the results were plotted in the form of complex plane diagrams (Nyquist plots). The frequency scan range was from  $1 \times 10^5$  to  $1 \times 10^{-1}\text{ Hz}$ , and the amplitude was 10 mV. All electrochemical measurements were performed at room temperature.

### Acknowledgements

This work was supported by the National Natural Science Foundation of China (No 20907051), the National High Technology Research and Development Program of China (2013AA065203), and the Knowledge Innovation Program of the Chinese Academy of Sciences (No DICP K2010C1).

**Keywords:** biosensors • electron transfer • mesoporous materials • nanostructures • phenolic chemicals



**Scheme 1.** Schematic representation of the preparation of the GMC/ $\text{Co}_3\text{O}_4$  nanocomposite-based Tyr biosensor and the biosensing mechanism.

a suspension of  $\text{Co}_3\text{O}_4$  ( $2.0\text{ mg mL}^{-1}$ ,  $10\text{ }\mu\text{L}$ ) and a solution of Chi ( $6.0\text{ mg mL}^{-1}$ ,  $10\text{ }\mu\text{L}$ ) were sequentially mixed into the above solution. Finally, an aliquot ( $4\text{ }\mu\text{L}$ ) of this mixture was cast onto the surface of a freshly polished GCE to prepare the GMC/ $\text{Co}_3\text{O}_4$ -Tyr-Chi/GCE biosensor, and then the electrode was dried at room temperature. When not in use, the fabricated electrode was stored in PBS at  $4^\circ\text{C}$  in a refrigerator.

Other enzyme electrodes were prepared by using procedures similar to those described above. A suspension containing GMC ( $0.2\text{ mg mL}^{-1}$ ), Tyr ( $2.5\text{ mg mL}^{-1}$ ), and Chi ( $1.5\text{ mg mL}^{-1}$ ) was used to prepare the GMC-Tyr-Chi/GCE biosensor. A suspension containing  $\text{Co}_3\text{O}_4$  ( $0.5\text{ mg mL}^{-1}$ ), Tyr ( $2.5\text{ mg mL}^{-1}$ ), and Chi ( $1.5\text{ mg mL}^{-1}$ ) was used to prepare the  $\text{Co}_3\text{O}_4$ -Tyr-Chi/GCE biosensor. A suspension

- [1] F. Karim, A. N. M. Fakhruddin, *Rev. Environ. Sci. Bio/Technol.* **2012**, *11*, 261–274.
- [2] Y. P. Neo, A. Ariffin, C. P. Tan, Y. A. Tan, *Int. J. Food Sci. Technol.* **2008**, *43*, 1832–1837.
- [3] D. Štěrbová, J. Vlček, V. Kubáň, *J. Sep. Sci.* **2006**, *29*, 308–313.
- [4] Q. Z. Feng, L. X. Zhao, W. Yan, J. M. Lin, Z. X. Zheng, *J. Hazard. Mater.* **2009**, *167*, 282–288.
- [5] L. Choueiri, V. S. Chedea, A. Calokerinos, P. Kefalas, *Food Chem.* **2012**, *133*, 1039–1044.
- [6] a) L. M. Lu, L. Zhang, X. B. Zhang, S. Y. Huan, G. L. Shen, R. Q. Yu, *Anal. Chim. Acta* **2010**, *665*, 146–151; b) W. Song, D. W. Li, Y. T. Li, Y. Li, Y. T. Long, *Biosens. Bioelectron.* **2011**, *26*, 3181–3186; c) L. J. Yang, H. Y. Xiong, X. H. Zhang, S. F. Wang, *Bioelectrochemistry* **2012**, *84*, 44–48.
- [7] S. Chawla, R. Rawal, S. Sharma, C. S. Pundir, *Biochem. Eng. J.* **2012**, *68*, 76–84.
- [8] J. Li, Z. J. Yang, Y. C. Zhang, S. H. Yu, Q. Xu, Q. S. Qu, X. Y. Hu, *Microchim. Acta* **2012**, *179*, 265–272.
- [9] Y. Wang, Y. M. Li, L. H. Tang, J. Lu, J. H. Li, *Electrochem. Commun.* **2009**, *11*, 889–892.
- [10] W. Chen, Y. Ding, J. Akhigbe, C. Bruckner, C. M. Li, Y. Lei, *Biosens. Bioelectron.* **2010**, *26*, 504–510.
- [11] J. Zhang, J. P. Lei, Y. Y. Liu, J. W. Zhao, H. X. Ju, *Biosens. Bioelectron.* **2009**, *24*, 1858–1863.
- [12] Z. J. Yang, X. C. Huang, R. C. Zhang, J. Li, Q. Xu, X. Y. Hu, *Electrochim. Acta* **2012**, *70*, 325–330.
- [13] S. Singh, D. V. S. Jain, M. L. Singla, *Anal. Methods* **2013**, *5*, 1024–1032.
- [14] a) W. Putzbach, N. J. Ronkainen, *Sensors* **2013**, *13*, 4811–4840; b) V. Scognamiglio, *Biosens. Bioelectron.* **2013**, *47*, 12–25; c) A. C. Chen, S. Chatterjee, *Chem. Soc. Rev.* **2013**, *42*, 5425–5438.
- [15] J. C. Ndamanisha, L. P. Guo, *Anal. Chim. Acta* **2012**, *747*, 19–28.
- [16] X. B. Lu, Y. Xiao, Z. B. Lei, J. P. Chen, H. J. Zhang, Y. W. Ni, Q. Zhang, *J. Mater. Chem.* **2009**, *19*, 4707–4714.
- [17] a) J. J. Feng, J. J. Xu, H. Y. Chen, *Biosens. Bioelectron.* **2007**, *22*, 1618–1624; b) M. Zhou, L. Shang, B. L. Li, L. J. Huang, S. J. Dong, *Biosens. Bioelectron.* **2008**, *24*, 442–447; c) L. D. Zhu, C. Y. Tian, D. X. Yang, X. Y. Jiang, R. L. Yang, *Electroanalysis* **2008**, *20*, 2518–2525.

- [18] M. I. Kim, Y. Ye, B. Y. Won, S. Shin, J. Lee, H. G. Park, *Adv. Funct. Mater.* **2011**, *21*, 2868–2875.
- [19] X. B. Lu, G. F. Zou, J. H. Li, *J. Mater. Chem.* **2007**, *17*, 1427–1432.
- [20] B. C. Janegitz, R. A. Medeiros, R. C. Rocha, O. Fatibello, *Diamond Relat. Mater.* **2012**, *25*, 128–133.
- [21] L. D. Wu, X. B. Lu, H. J. Zhang, J. P. Chen, *ChemSusChem* **2012**, *5*, 1918–1925.
- [22] a) L. Cui, J. Li, X. G. Zhang, *J. Appl. Electrochem.* **2009**, *39*, 1871–1876; b) G. X. Wang, X. P. Shen, J. Horvat, B. Wang, H. Liu, D. Wexler, J. Yao, *J. Phys. Chem. C* **2009**, *113*, 4357–4361.
- [23] Y. W. Hu, F. H. Li, X. X. Bai, D. Li, S. C. Hua, K. K. Wang, L. Niu, *Chem. Commun.* **2011**, *47*, 1743–1745.
- [24] a) H. Faridnouri, H. Ghourchian, S. Hashemnia, *Bioelectrochemistry* **2011**, *82*, 1–9; b) A. B. Moghaddam, M. R. Ganjali, M. Niasari, S. Ahadi, *Anal. Lett.* **2008**, *41*, 3161–3176.
- [25] M. M. Rahman, A. J. S. Ahammad, J. H. Jin, S. J. Ahn, J. J. Lee, *Sensors* **2010**, *10*, 4855–4886.
- [26] R. F. Gao, J. B. Zheng, *Electrochem. Commun.* **2009**, *11*, 608–611.
- [27] E. Laviron, *J. Electroanal. Chem.* **1979**, *101*, 19–28.
- [28] Q. Ameer, S. B. Adeloju, *Sens. Actuators B* **2009**, *140*, 5–11.
- [29] M. Portaccio, D. Di Tuoro, F. Arduini, M. Lepore, D. G. Mita, N. Diano, L. Mita, D. Moscone, *Biosens. Bioelectron.* **2010**, *25*, 2003–2008.
- [30] A. Arecchi, M. Scampicchio, S. Drusch, S. Mannino, *Anal. Chim. Acta* **2010**, *659*, 133–136.
- [31] C. Apetrei, M. L. Rodriguez-Mendez, J. A. De Saja, *Electrochim. Acta* **2011**, *56*, 8919–8925.
- [32] R. X. Han, L. Cui, S. Y. Ai, H. S. Yin, X. G. Liu, Y. Y. Qiu, *J. Solid State Electrochem.* **2012**, *16*, 449–456.
- [33] S. Hashemnia, S. Khayatzaadeh, M. Hashemnia, *J. Solid State Electrochem.* **2012**, *16*, 473–479.
- [34] X. R. Li, T. K. Ren, N. Wang, X. P. Ji, *Anal. Sci.* **2013**, *29*, 473–477.
- [35] S. Singh, D. V. S. Jain, M. L. Singla, *Sens. Actuators B* **2013**, *182*, 161–169.
- [36] D. Du, M. H. Wang, J. Cai, Y. H. Qin, A. D. Zhang, *Sens. Actuators B* **2010**, *143*, 524–529.
- [37] T. Yokoi, Y. Sakamoto, O. Terasaki, Y. Kubota, T. Okubo, T. Tatsumi, *J. Am. Chem. Soc.* **2006**, *128*, 13664–13665.
- [38] J. Du, L. L. Chai, G. M. Wang, K. Li, Y. T. Qian, *Aust. J. Chem.* **2008**, *61*, 153–158.

---

Received: October 30, 2013

Published online on March 18, 2014